Supporting Information

An etching-templating dual strategy for the *in situ* synthesis of carbon-supported iron metaphosphate and application as electrocatalyst

*Jingbo Huang, Junzheng Wei, Wei Sang, Qifu Zhang, Yongda Guo and Yating Hu**

Outline

1. Experimental Section

2. Figures

3. Tables

4. References

1. Experimental Section

***Chemicals*:** Iron chloride hexahydrate ($FeCl_3.6H_2O$, Macklin, 99%), Sodium hydroxide ($NaOH$, AR), n-Hexylphosphonic acid (HPA, Macklin, 98 %), Lauric acid ($C_{12}H_{24}O_2$, Macklin, 98 %), n-Hexane (C_6H_{14}, Macklin, ≥98 %, GC), N, N-Dimethylfornanide (DMF, Macklin, 99.5 %), Nafion® perfluorinated resin-aqueous dispersion (Aladdin, 5 wt.% in water), Carbon black (Macklin, xc-72R, 10-20 nm) and ethanol (CH_3CH_2OH, Macklin, 95 %), commercial platinum carbon catalysts (Pt/C, 20wt. % Pt supported on carbon black).

***Synthesis of Fe_3O_4 nano-size octahedra*:** Fe_3O_4 nano-size octahedra was synthesized following a hydrothermal method reported by Zong et al.[1]

***Synthesis of Fe-HPA*:** 1 mmol of Fe_3O_4 nano-size octahedra was dispersed and ultrasonicated in 6 ml of n-hexane for 30 min. Subsequently, 8 mmol of HPA and 30 g of lauric acid were added. The mixture was heated to 60 ℃ under vigorous stirring, with N_2 gas purged it for 1 hour to degas and remove n-hexane and air. Then, the Fe_3O_4 nano-size octahedra and HPA in lauric acid solution were heated up to 295 ℃ under N_2 atmosphere and refluxed at this temperature for 8 h. After heating was completed, large amount of dark brown precipitate is observed. The mixture was cooled to 60 ℃, followed by the addition of 40 ml DMF and stirring. DMF is used to dissolve lauric acid residue from the synthesized Fe-HPA product, as solidifies at room temperature. Fe-HPA precipitates was then collected by centrifugation. The precipitates were washed by DMF for 2 times and ethanol for 1 time to remove the residues of HPA and lauric acid. After drying in oven at 60 ℃ and grinding treatment, a grey powder was

collected.

Synthesis of Iron (II) metaphosphate

Single-Step Heat Treatment: The as-synthesized Fe-HPA powder was placed in an alumina crucible and then placed in a tube furnace for heat treatment under N_2 atmosphere until the furnace was cooled down to below 100 ℃.

***Two-Step Heat Treatmen*t**: Step1 (vacuum pyrolysis). The as-synthesized Fe-HPA powder was placed into an alumina crucible and then placed in the same tube furnace as like the *single-step heat treatment.* During the vacuum pyrolysis, the vacuum level was maintained at ~ 4×10^{-4} mbar by using a mechanical pump and a turbo pump together. After holding period, the cooling process was conducted under N_2 atmosphere. Step 2 (annealing process). The product from Step 1 was retrieved, ground into fine powder, and re-placed into the crucible. This was then transferred back into the tube furnace for short-term annealing under N_2 atmosphere.

***Material Characterizations*:** The samples were analyzed using X-ray diffraction (XRD), transmission electron microscopy (TEM), Scanning electron spectroscopy (SEM), Energy-dispersive X-ray analysis (EDX), Thermal gravimetric analysis (TGA), N_2 adsorption/desorption, Raman spectroscopy and Fourier transform infrared (FTIR) spectroscopy. XRD patterns were obtained using a SmartLabTM 9 kW X-ray diffractometer (Cu Kα radiation, λ=1.541 Å) and with the scan rate of 10 °/min. TGA was done using SDT Q600 under N_2 from room temperature to 600 °C with 5 °C/min ramp rate. N_2 adsorption/desorption was done at 77 K using Micromeritics ASAP 2460 instrument; degas treatment: heated from room temperature to 160 °C at 5 °C/min ramp

rate and degassed for 12 h. SEM images were captured using a FEI Apreo C microscope, allowing for high-resolution imaging and analysis of the samples. TEM characterization were performed on a FEI Talos F200S 200 kV transmission electron microscope, coupled with a Super-XEDS for dispersive X-ray spectroscopy (EDS) and elemental mapping.

***Electrochemical measurements and calculations*:** Oxygen reduction reaction (ORR) catalytic activity and electrical impedance spectroscopy (EIS) of the samples were tested in a standard three-electrode system in 0.1 M KOH solution (PH=13.45), using a Pine WaveDriver 200. An Ag/AgCl electrode and a graphite rod were used as the reference electrode and counter electrode, respectively. Preparation of working electrodes: 2 mg of catalysts and 6 μl of Nafion 117 solution (5 wt. %) were uniformly dispersed in 1 mL of carbon black dispersion (a mixture of 2 mg carbon black and 10 ml ethanol, with a concentration of 0.2 mg/ml for carbon black) by using ultrasonication for 1 h. 50 μl of the dispersion was then dropped on the rotating disk electrode (RDE), or glassy carbon electrode (GCE) with a geometric area of 0.196 cm^2 and the loading of material on them was about 0.51 mg cm^{-2}. The EIS was tested with a conventional three-electrode system by an IVIUM Vertex, across a frequency range of 10^5 to 0.1 Hz. ORR curves were collected at rotation rates ranging from 400 to 2000 rpm and the curve at 1600 rpm was used to obtain the onset potential (the tangent point where a tangent line is drawn at the intersection of the liner region and the reaction region in the i-E curve) and the scan rate was kept constant at 10 mV/s for all the Cyclic voltammetry (CV) and Linear sweep voltammetry (LSV) experiments. Unless otherwise mentioned,

20 cycles of pre-CV curves were collected at 50 mV/s in N_2-saturated solution before conducting CV/LSV testing for activation and stabilization purposes. The electron transform number *n* was calculated based on the slopes of the Koutecky-Levich plots and Koutecky-Levich equation:

$$j_k = nFAD^{2/3}v^{-1/6}C^*$$

j_k: Limiting diffusion current density (A/cm²)

A: Electrode area (cm²)

D: Reactant diffusion coefficient (cm²/s)

v: Kinematic viscosity of the electrolyte (cm²/s)

C^*: Bulk concentration of the reactant (mol/cm³)

To further verify the average number of electrons exchanged (*n*) and the formation of byproducts, we also prepared 50 μl of the dispersion on the rotating ring-disk electrode (RRDE) for RRDE measurements. The RRDE measurements were performed in 0.1 M KOH solution and the LSVs were recorded at 10 mV/s between -1.0 and 0.25 V vs. Saturated Calomel Electrode (SCE) under N_2- and O_2- saturated electrolytes. The ring electrode was held at 1.3 V vs. Reversible Hydrogen Electrode (RHE) during the ORR measurements with the RRDE rotation rate of 1600 rpm. The hydrogen peroxide yield ($H_2O_2\%$) and *n* during the ORR were determined by RRDE technique and calculated via the following equations (*N*=0.37):

$$H_2O_2(\%) = 200 \times \frac{\frac{I_r}{N}}{I_d + \frac{I_r}{N}}$$

$$n = 4 \times \frac{I_d}{I_d + \frac{I_r}{N}}$$

I_d: Disk current (A)

I_r: Ring current (A)

N: Current collection efficiency

2. Figures

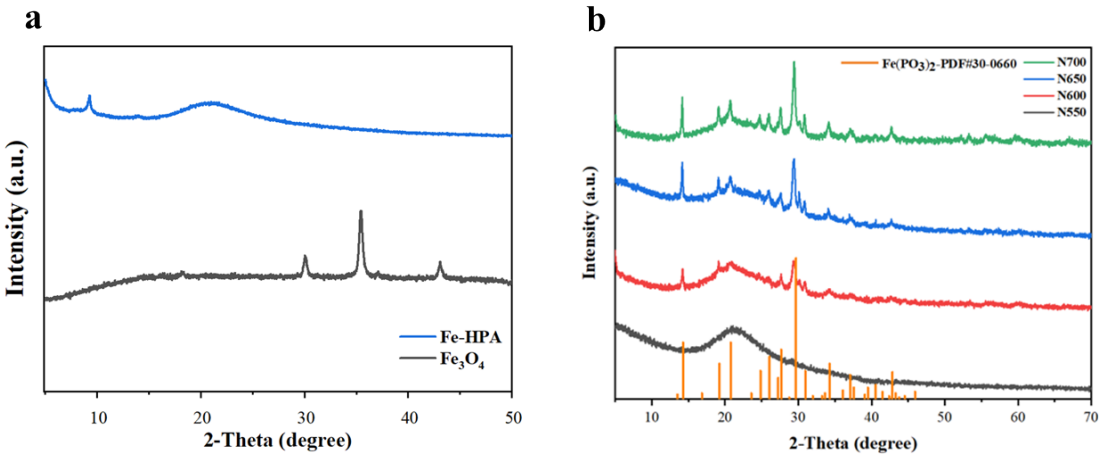

Figure S1. XRD patterns of (a) Fe_3O_4 precursor and Fe-HPA and (b) N550, N600, N650 and N700.

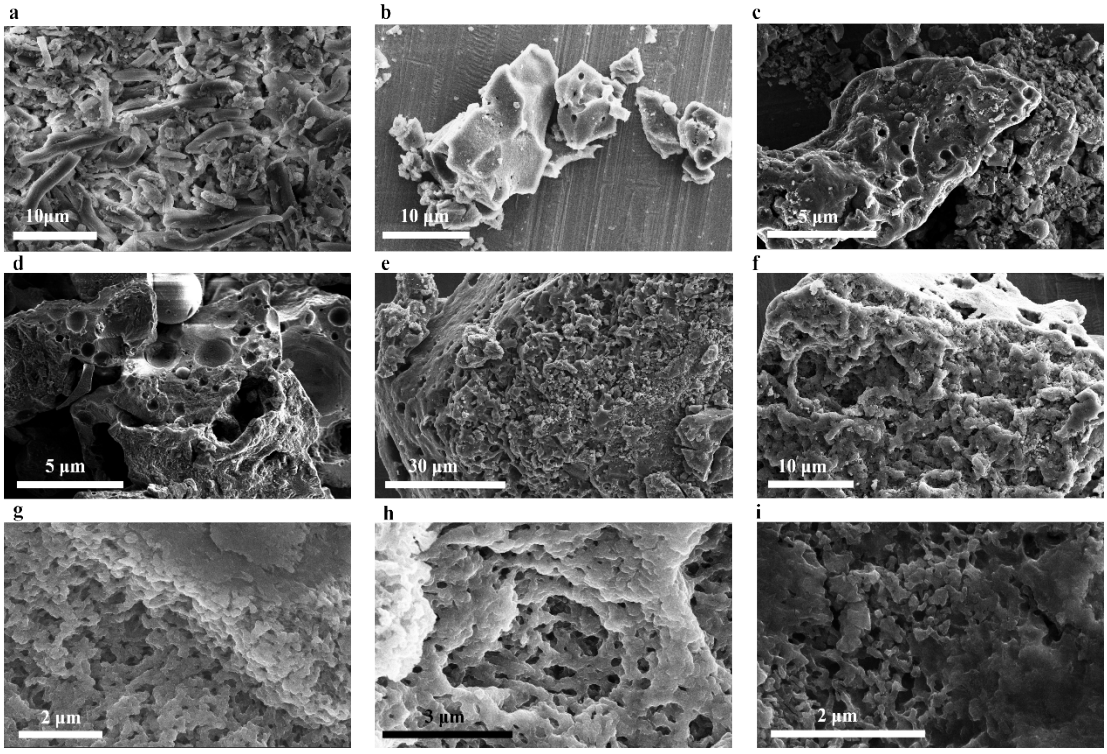

Figure S2. SEM images of (a) Fe-HPA, (b) N550, (c) N600, (d)N650, (e) V450-N650, (f) V450-N700, (g) V450-0.5h, (h) V500-1.5h and (i) V550-1h.

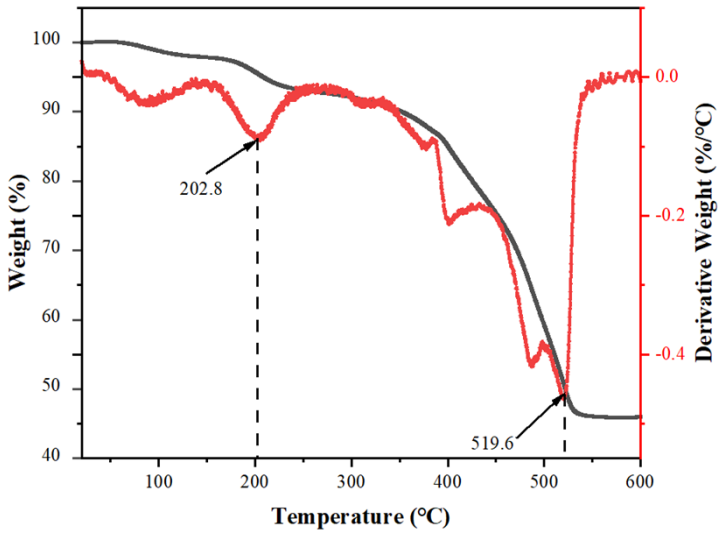

Figure S3. TGA and derivative thermogravimetry (DTG) curves for Fe-HPA pyrolyzed in N_2 at the rate of 5 °C min^{-1}.

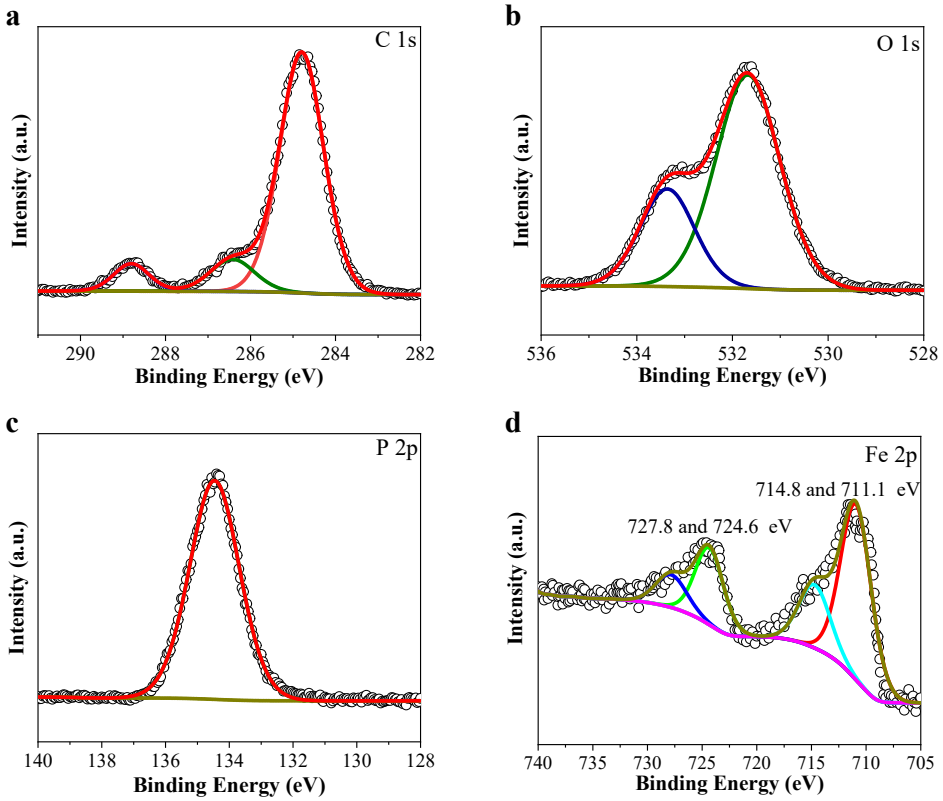

Figure S4. X-ray photoemission spectrum (XPS) spectrum of N700: (a) C 1s, (b) O 1s, (c) P 2p and (d) Fe 2p.

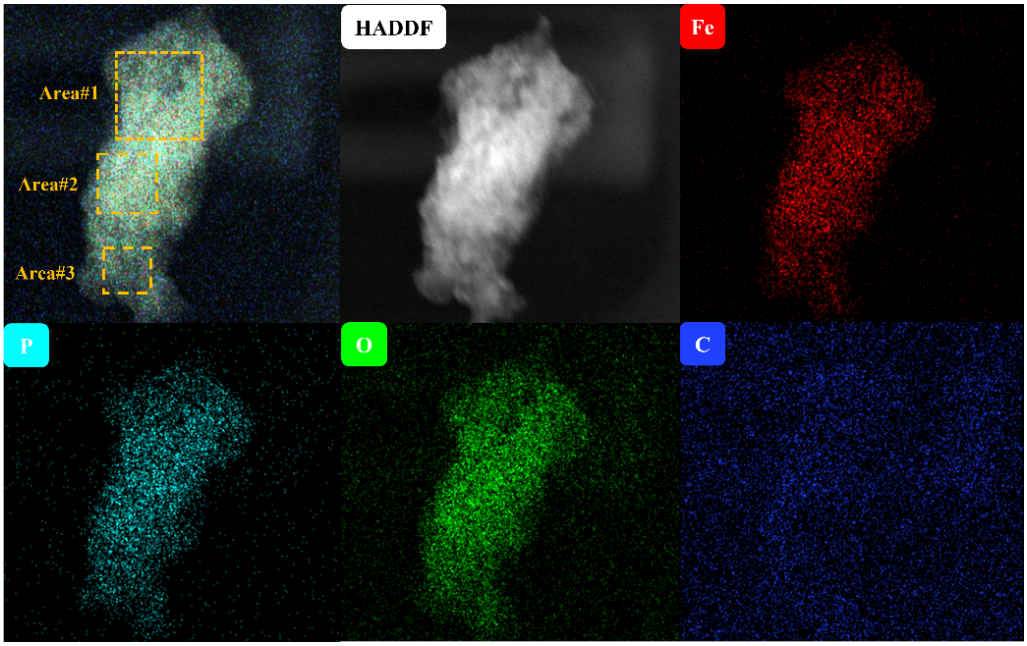

Figure S5. Energy-dispersive X-ray spectroscopy (EDS) images of V450-N700.

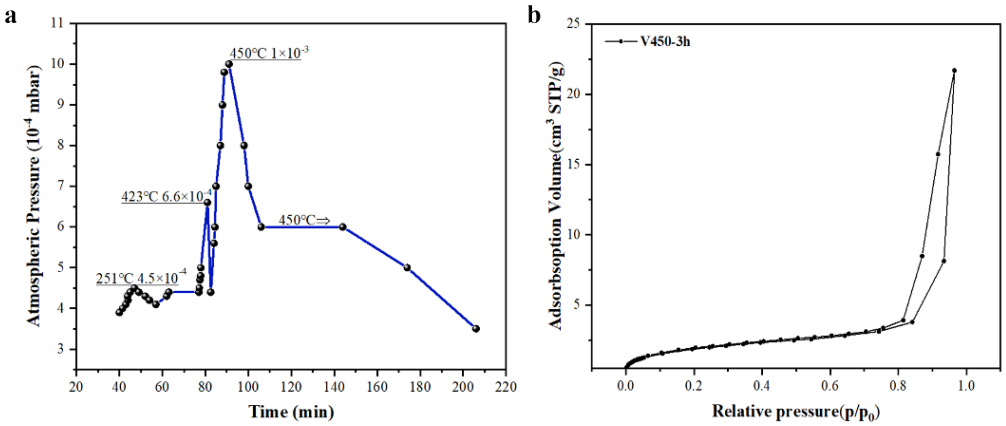

Figure S6. (a) Atmospheric pressure trend during vacuum pyrolysis and (b) N_2 adsorption isotherm of V450 (BET specific surface area of 7.0 m^2/g) .

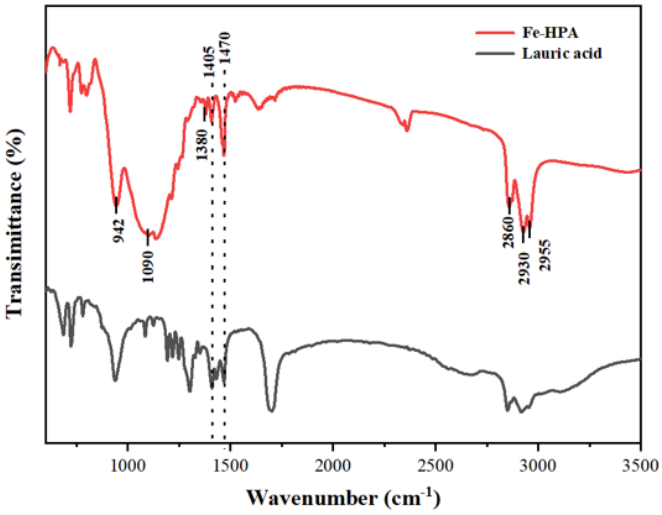

Figure S7. FTIR spectroscopy of Fe-HPA and lauric acid.

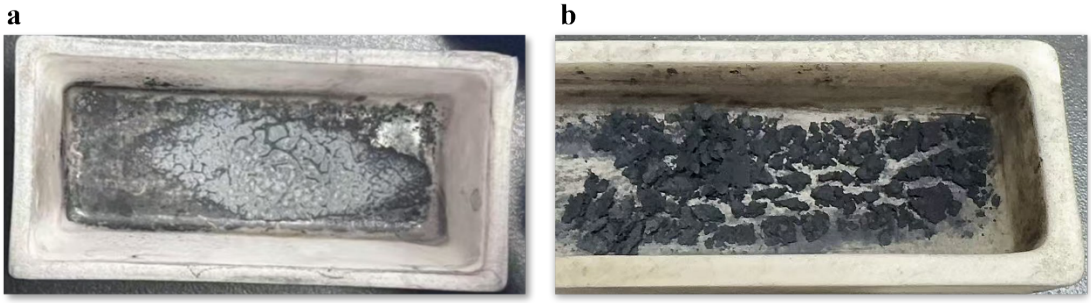

Figure S8. Picture showing the color and macroscopic morphology differences between (a) N450 and (b) V450.

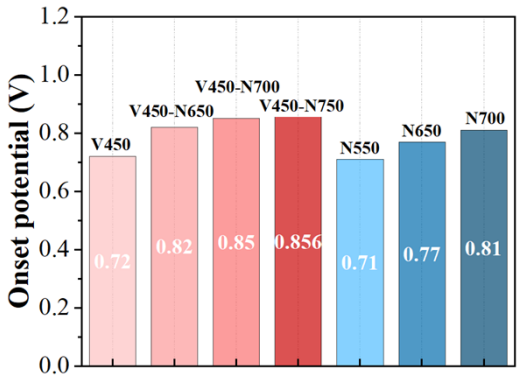

Figure S9. The Onset potential value for various samples.

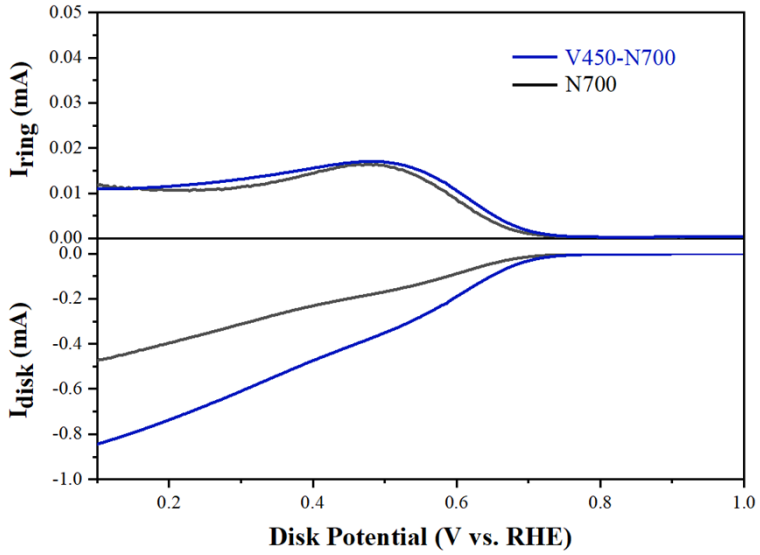

Figure S10. Disk and ring current as a function of the disk potential for V450-N700 and N700.

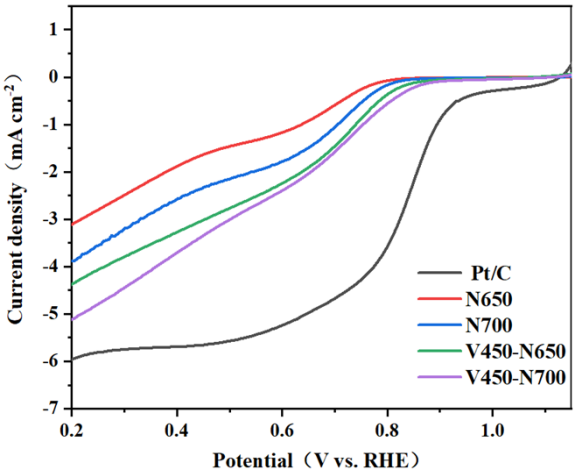

Figure S11. LSV curves of ORR for Pt/C and various samples under vacuum or N_2 atmospheres (N650, N700, V450-N650, N450-N700).

3. Tables

Table S1. Nomenclature and heat-treatment conditions for various samples. V or N-series indicate the single step treatments under vacuum or nitrogen. V-N series indicate the two-step treatments.

Sample Name	Temperature (°C)	Holding time (h)	Atmosphere

V450	450	3	Vacuum
V450-N600	600	1	N_2
V450-N650	650	1	N_2
V450-N700	700	1	N_2
V450-N750	750	1	N_2
N450	450	3	N_2
N550	550	3	N_2
N600	600	3	N_2
N650	650	3	N_2
N700	700	3	N_2
V450-0.5h	450	0.5	Vacuum
V500-1.5h	500	1.5	Vacuum
V550-1h	550	1	Vacuum

Table S2. Crystallite size calculations via Scherrer equation (k=0.9, λ=1.54 Å).

Name	peak	2θ	θ	cosθ	FWHM	FWHM in Rad	Crystal size (nm)	Average (nm)
N700	1	29.41	14.705	0.967	0.448	0.00781	183.48	**176.41**
	2	30.15	15.705	0.965	0.515	0.00899	159.71	
	3	34.14	17.07	0.955	0.447	0.00779	186.05	
N750	1	29.45	14.725	0.967	0.507	0.00886	161.89	**197.15**
	2	30.27	15.135	0.965	0.317	0.00554	259.43	
	3	34.22	17.11	0.955	0.489	0.00853	170.13	
V450-N700	1	29.42	14.71	0.967	0.570	0.00995	144.06	**113.88**
	2	30.21	15.105	0.965	0.682	0.01190	120.71	
	3	34.8	17.4	0.954	1.083	0.01891	76.86	
N450-N750	1	29.34	14.67	0.967	0.504	0.00879	162.99	**119.50**
	2	30.16	15.08	0.965	0.712	0.01242	115.59	
	3	34.68	17.34	0.955	1.041	0.01817	79.93	

Table S3. Element contents of different areas in Figure S3.

	Fe at%	P at%	O at%	C at%
Area #1	11.18	10.25	51.76	26.8
Area #2	10.04	9.01	48.47	32.48
Area #3	23.08	12.9	37.17	26.85

Table S4. Mass loss data of V450 and N450.

Sample	Initial Mass (mg)	Final Mass (mg)	Mass Remains
V450	206	56	27.2%
N450	54	18	33%

Table S5. ORR performance of the non-noble electrocatalysts.

Catalyst	Electrolyte	Onset-potential (V vs. RHE)	Ref
Carbon Black (Macklin, xc-72R)	0.1M KOH	0.69	Tested in this work.
Co-N/C	0.1M KOH	0.85	[2]
$Mn(PO_3)_2$-C	0.1M KOH	0.87	[3]
FeP/PC	0.1M KOH	0.873	[4]
Fe-N-C	0.1M KOH	0.98	[5]

References

1. Y. Zong, H. Xin, J. Zhang, X. Li, J. Feng, X. Deng, Y. Sun and X. Zheng, *Journal of Magnetism and Magnetic Materials*, 2017, **423**, 321-326.
2. L. An, W. Huang, N. Zhang, X. Chen and D. Xia, *Journal of Materials Chemistry A*, 2014.
3. MinZhou, JinghuiGuo, RuihuLu, JiantaoLi, SungsikLee, ChunhuaHan, XiaobinLiao, PingLuo, YanZhao and ZhaoyangWang, *Interdisciplinary Materials*, 2024, **4**, 309-320.
4. X. Lian-Hua, C. Peng-Cheng, Z. Xue-Ji, C. Serge and S. Dan, *Applied Surface Science*, 2023, **620**.
5. B. Hou, C. C. Wang, R. Tang, Q. Zhang and X. Cui, *Materials Research Express*, 2020, **7**, 025506-025506.